

# Fundamental research on the property assessment of ground improvement utilizing the borehole wall imaging

Yasunori OOTSUKA<sup>(1)</sup>, Hirokazu YASUTOMI<sup>(2)</sup>, Katsuhiro TAJIMA<sup>(3)</sup> and Omer AYDAN<sup>(4)</sup>

(1) Earth Scanning Association, Japan

E-mail:y.ootsuka@esa.gr.jp

(2) Nippon Geophysical Prospecting Co, Japan,

(3) Earth Scanning Association, Japan, (4) University of the Ryukyus, Japan

## Abstract

In the field of ground improvement, various construction techniques have been developed to produce homogeneous solidified columns of well-defined dimension and strength. The uniaxial compression strength obtained from laboratory soil tests of boring cores after the formed piles have been hardened is generally used to verify and control the quality of the improvement piles. However, there is demand for techniques to quickly and continuously identify the physical properties and mechanical properties associated with the improvement piles that have been formed. In this study, we acquired borehole wall images through inserting optical and ultrasonic borehole image scanner in the boring holes excavated in the improvement piles that have been experimentally constructed, and have conducted uniaxial compression tests using the boring cores of the improvement piles. We were able to continuously identify the shape and the distribution of both the void areas (unconsolidated areas) and the solid areas (mixture of cement milk and soil in-situ). In addition, a trend similar to that found between the porosity and the uniaxial compression strength of the core specimen was also observed in the ultrasonic wave reflection intensity of the borehole wall and the uniaxial compression strength of the core specimen. As a result, it was suggested that it may be possible to quickly and continuously identify the uniaxial compression strength of the improvement piles by means of the ultrasonic wave reflection intensity from the borehole walls.

**Keywords:** ground improvement pile, borehole image scanner, porosity, ultrasonic wave reflection intensity

## 1. Introduction

Ground improvement is a soft soil stabilization method which mixes soft soil in-situ with solidified material such as cement to produce soil-cement with higher strength than the soil in-situ. As part of the overall quality control for improved soil, we generally verify that the target value for improvement is reached upon the uniaxial compression strength of the boring cores which we collect after the formed piles finish hardening. However, it is difficult to continuously monitor and maintain awareness of the strength since laboratory soil tests are limited in the area which is hardened to the extent that it is possible to shape the test specimen.

Therefore, in this study, we carried out core boring on four improvement piles, which were inclusive of both hard and soft consistencies that were formed under the test construction, and we

obtained borehole image data using optical and ultrasonic borehole image scanner in the boring holes. The results from the laboratory soil tests of the core specimens exhibited a good correlation between the porosity of the improved soil and the uniaxial compression strength. In addition, the results of the image analysis using the borehole wall image data displayed a good correlation between the uniaxial compression strength of the core specimen and the ultrasonic wave reflection intensity of the borehole walls. The results indicate that it is possible to continuously and quickly monitor and maintain awareness of the uniaxial compression strength of the improved soil based on the borehole wall image data. Some of the results of this research have been presented at the ARMS8 by Kawakami et al. (2014).

## 2. Features of borehole image scanner

The components for ODS (Optical Digital

Scanner) system and USS (Ultra Sonic Scanner) system of borehole image scanner are shown in Fig. 1. As shown in the figure, both systems consist of probe, controller, depth encoder, remote control winch and a note pc. Except the probe and the controller, all the other parts are common, so it is very convenient to change the system from one to another by only substituting the probe and the controller.

Specifications of both the ODS and USS are shown in Table 1. As shown in the table, the controller is operable in air temperature from 0 to 40°C, enabling its application in most region of the

world.

The ODS probe is operable in temperature from 0 to 40°C and the USS probe even can be operated from 0 to 50°C, so the probe can be used in most non-geothermal area. The USS probe can be used in borehole of diameters from 56 to 148mm while the ODS probe can be used in borehole from 56mm to 200mm in diameter. The 300m winch enables the system to be used in most boreholes for civil engineering purpose. Especially, ultrasonic borehole image scanner details have been reported by Sato et al. (2009) and Kawakami et al. (2009).

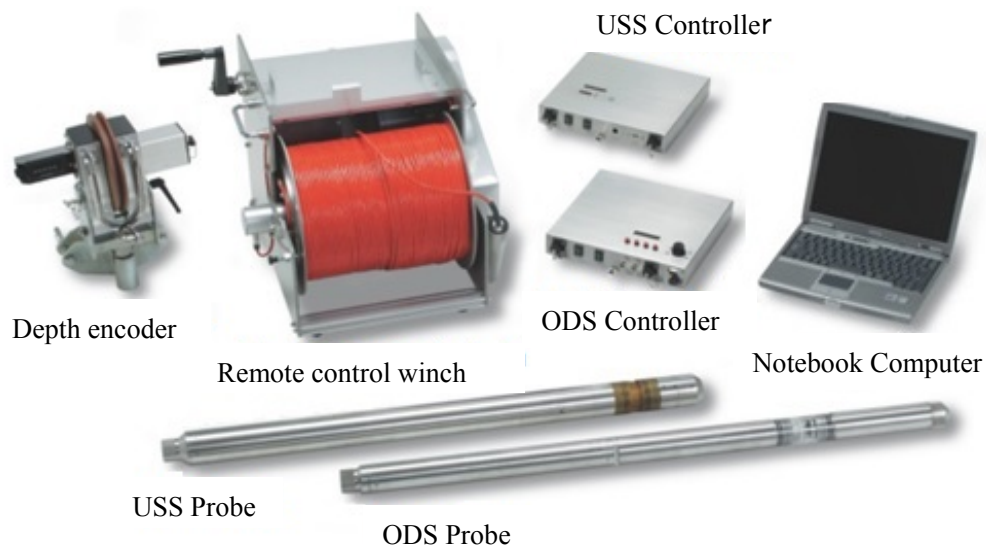


Fig. 1 System components for ODS and USS

Table 1 Specification of borehole image scanner

Article	Items	ODS (Optical Digital Scanner)	USS (Ultra Sonic Scanner)
Controller	Operation temperature	0~40° C (without moisture)	
	Power supply	AC100V (ODS 200m system AC240V available)	
	Size	272 ×252×45 mm	
	Image output	NTSC (RCA connector ) USB 2.0	
Probe	Operation temperature	0~40° C (without moisture)	0~50° C
	Water proof	500m	
	Borehole diameter	φ 56mm ~ φ 200mm	φ 56mm ~ φ 148mm
	Size	φ 50mm L = 1030mm	φ 50mm L = 930mm
	Resolution	depth 0.25mm (min)	depth 0.25mm (min)
		horizontal 360/720pixel	horizontal 360pixel
	Ground water	water or dry condition	water condition
	Peformance	Borehole projected image 180/360degree	frequency 1.0 MHz
		built -in orientation sensor	
		full color	black and white
Winch	Sensor rotation	no rotation	600 revolutions/min
	Length	200m & 300m	
	Cable	5 core,kevlar cable	
Others	Operation	PC	
	Saving data	HDD/external video recorder	HDD
	Depth pulse encoder	0.25mm/Pulse	
	Survey speed	0~216m/ h(standard 54m/h)	0~36m/h

### 3. Overview of field tests

We thought it ideal to use man-made soil that had some variation in hardness as the target soil for this field test. Therefore, we decided to use four test improvement piles. We knew in advance that these piles had some variation in uniaxial compression strength due to being formed changing agitating and mixing specifications.

The construction conditions varied for each of the improvement piles which were experimentally

formed in a manner so that we could see the effects associated with the specification of mechanical performance and mixing means, targeting volcanic cohesive soil as shown in Table 2. The period in which these improvement piles were formed was approximately half a year prior to the field measurements performed in this study. We collected boring cores in the position about 0.4 m (half of the radius) away from the center of the ground improvement pile and acquired borehole wall images with ODS and USS equipment in the same borehole.

Table 2 Construction conditions and test results for the ground improvement piles

Items		CASE 1	CASE 2	CASE 3	CASE 4
Construction conditions	Target Soil Type	Volcanic cohesive soil			
	Cement Adding Quantity	250 kg/m <sup>3</sup>			
	Improved depth	7.0m			
	Improvement of Smooth Rotation	Absence		Presence	
	Drawing Speed	Low	High	Low	High
Test results of the cores after piles were formed	Core Solidification	○	△ (including some unconsolidated parts )	○	△ (including some unconsolidated parts )
	Variation of Uniaxial Compression Strength	The solidified area satisfies the target strength of 500 kN/m <sup>2</sup> (Strength on 28th day)			
		Slightly large		Small	Slightly large

#### 4. Relationship between physical and mechanical property

Physical and mechanical laboratory tests are performed using the boring cores. Fig. 2 shows the relationship between the wet density and the uniaxial compression strength, and Fig. 3 shows the relationship between the porosity and the uniaxial compression strength. From both of these figures, we can see general relationships in which the uniaxial compression strength increases in conjunction with increases in wet density, and increases in conjunction with decreases in porosity.

Fig. 4 shows an example of both ODS and USS borehole wall image which were measured in the same respective location. The waveforms shown on the right side are depictive of ultrasonic reflection waveforms obtained at the circles in the USS image.

We show the maximum reflection intensity in a grayscale with 256 shades. The lighter shades of gray depict higher reflection intensity, whereas the darker shades of gray depict lower reflection intensity.

The ODS image shows multiple clumps of void area (unconsolidated area) that were left behind during the consolidation process. These clumps of soil appear to be darker on the USS image due to the texture being softer than that found in the improved and hardened clumps of soil. In addition, the traces of scratches running in a vertical direction that were thought to be formed when the boring core tubes were moving up and down were indistinct on the ODS image. It is suggested that we can know the difference of both hardness and asperity of the borehole wall by USS image.

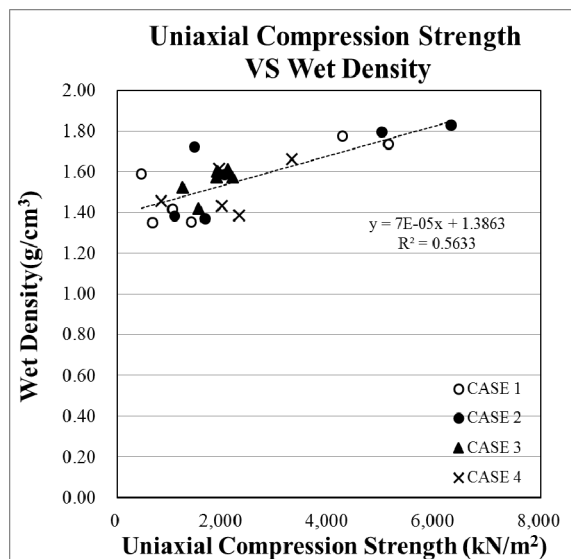


Fig.2 Relationship between uniaxial compression strength and wet density

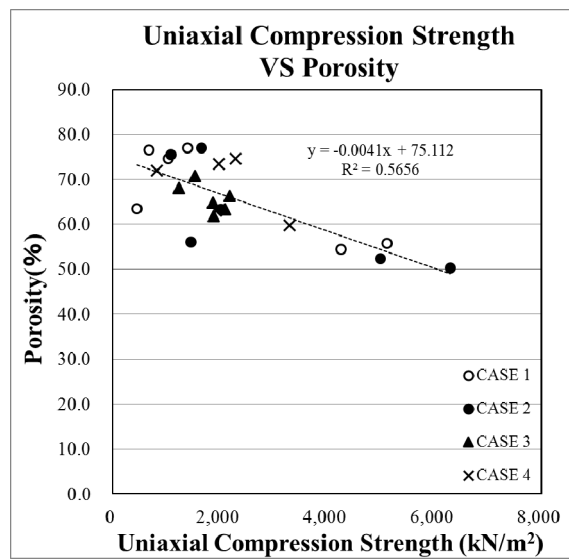


Fig.3 Relationship between uniaxial compression strength and porosity

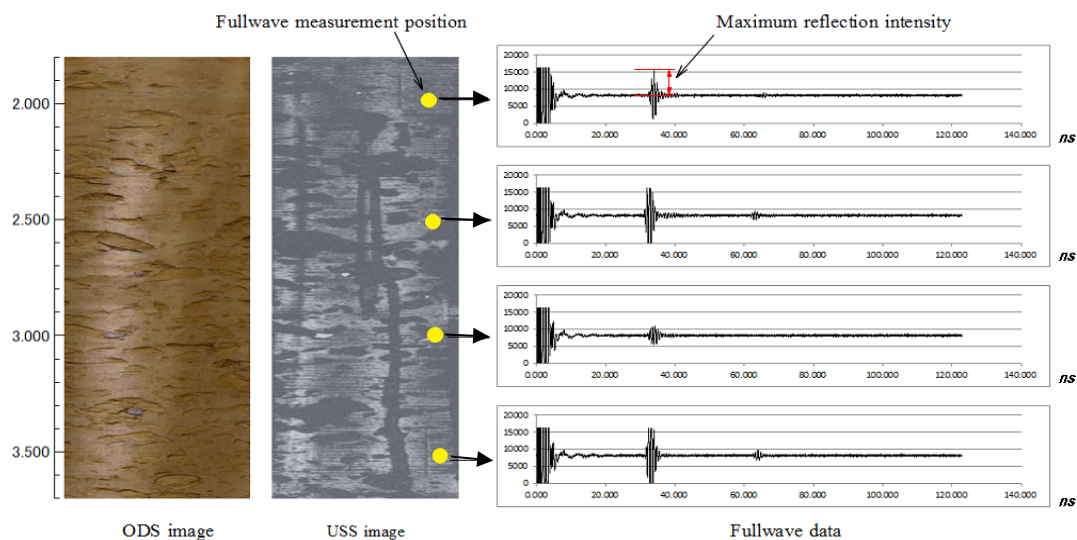


Fig.4 Comparison of ODS and USS borehole image with reflection intensity of USS

Next, Fig. 5 shows the changes in the ultrasonic wave reflection intensity and the uniaxial compression strength in the depth direction. The ultrasonic wave reflection intensity is depicted as an average value taken from 10 cm length of the entire circumference ( $360^\circ$ ) on the borehole wall, which is defined as circumferentially averaged reflection intensity. From Fig. 5, we can see a trend of increases in the uniaxial compression strength and the ultrasonic wave reflection intensity as we move towards the bottom of the boreholes in Case 1, Case 2, and Case 4. However, in Case 2, the ultrasonic

wave reflection intensity decreased in the areas with depths between 5.5 m and 6.5 m, whereas the uniaxial compression strength conversely increased. This is seemed to be due to the reflection intensity decreasing in response to the diffuse reflections by the turbidity of slime suspension near the bottom of the borehole. In contrast, in Case 3, we can see the constant reflection intensity and uniaxial compression strength from the ground surface to the bottom of the borehole. This is due to the difference of construction conditions as shown in Table 2.

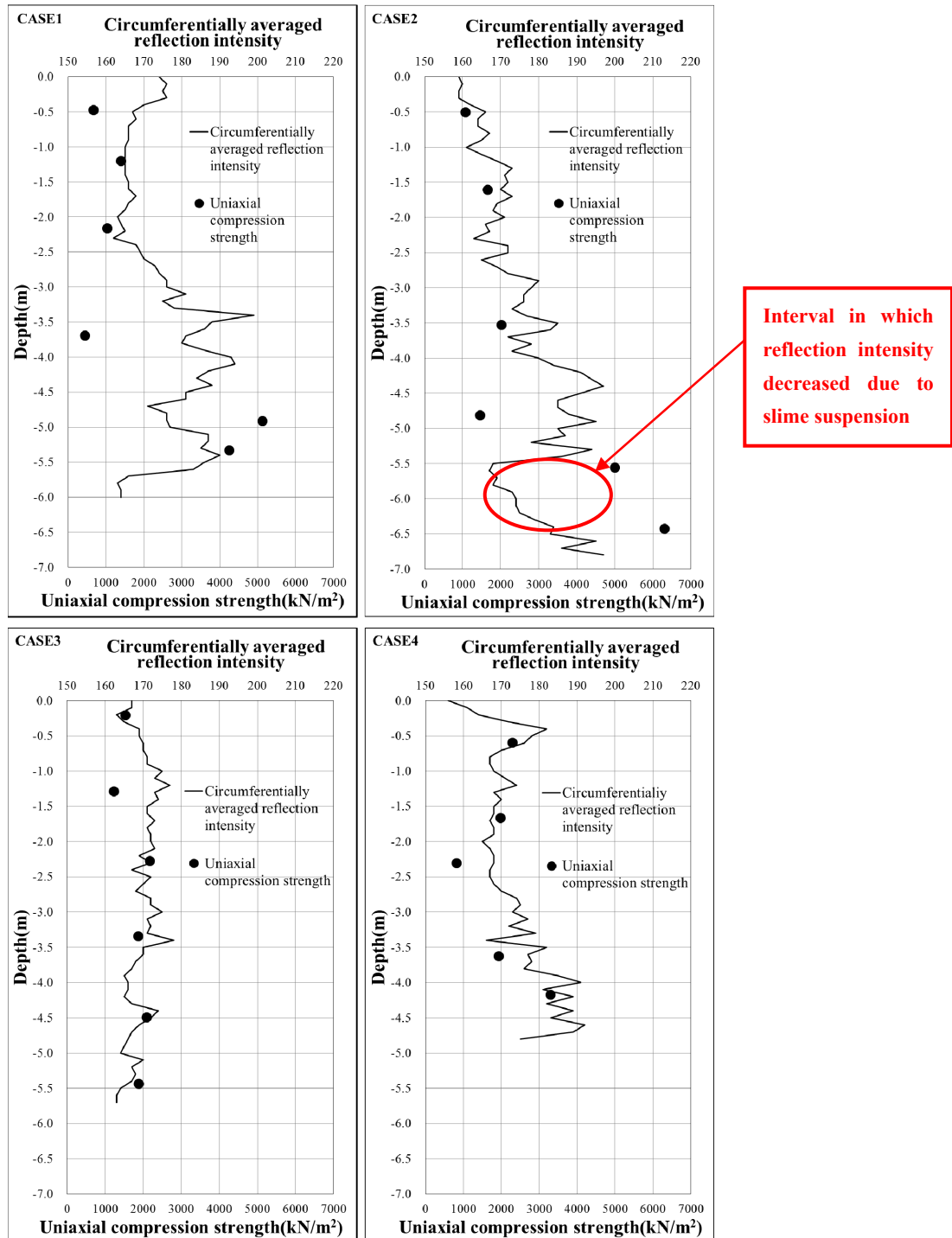


Fig.5 Relationship between reflection intensity and uniaxial compression strength in the depth

Fig. 6 shows the relationship between the uniaxial compression strength and the ultrasonic wave reflection intensity. The circumferentially averaged reflection intensity for the section where the core specimens (length=10cm, diameter=5cm) for laboratory tests were collected was used to see the relationship between the uniaxial compression strength and the ultrasonic wave reflection intensity. In the relationship diagram shown in Fig. 6, we don't use two sets of uniaxial compression strength data in Case 2 since the ultrasonic wave reflection intensity was very low due to slime suspension in the deep area. From this figure, although there was a variance especially within the area of high reflection intensity, we can see a tendency that the uniaxial compression strength increases in conjunction with increase in the ultrasonic wave reflection intensity. The significant variance in the data is due to void area (unconsolidated area) which was left behind in the improved clumps. If there is a hard consolidated area in the rear side, the uniaxial compression strength of the core specimen will increase. It is seemed to be one of the reasons of fluctuations.

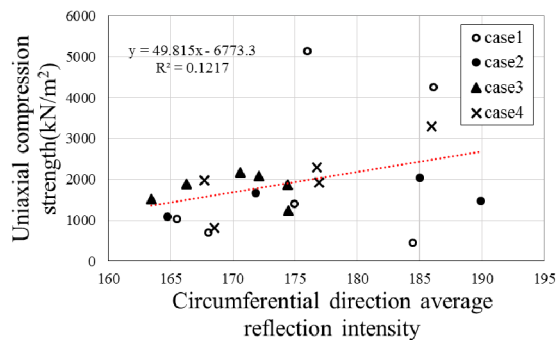


Fig.6 Relationship between circumferential direction average reflection intensity and uniaxial compression strength

## 5. Conclusions

In this study, we performed field measurements using optical (ODS) and ultrasonic (USS) borehole image scanner in the boring holes in addition to performing uniaxial compression tests as a means to confirm the quality of the ground improvement piles which were made by changing mechanical agitating and mixing treatment conditions. The results showed a good correlation between the porosity (volume ratio of unsolidified soil) and the uniaxial compression strength of the core specimen. Moreover, we found a similar correlation between the circumferentially averaged reflection intensity of ultrasonic wave from the borehole wall and the uniaxial compression strength of the core specimen. This indicates the feasibility of a technique that can quickly and continuously assess the quality of the ground improvement piles, complementing uniaxial

compression tests. Hereafter, we are going to further develop our research in establishing more effective assessment techniques for the ground improvement pile due to borehole wall images.

## Acknowledgements

In this study, we received a great deal of support from Raax Co., Ltd with regard to measurements and equipment to perform these field experiments using borehole image scanner. Additionally, Dr.Naohiko Tokashiki from the University of the Ryukyus provided valuable feedback with regard to the direction in which we further develop this research in future. Finally, we would also like to express our deep gratitude and thanks to all of those who provided support to this research.

## References

- Kawakami,A., Yasutomi,H., Murata,A., Nakahara,T., Hiraki,H., Moriguchi,Y., Ootsuka,Y. and Tajima,K. (2014): Comparison of Borehole Scanning Systems, Optical Digital Scanner (ODS) and Ultrasonic Scanner (USS) , Proceedings of 8th Asian Rock Mechanics Symposium,ISRM, pp. 2224-2232
- Sato,S. and Katusima,N.(2009): Some examples of ground evaluation by ultrasonic borehole scanner (in Japanese) , Geotech e-forum2009, Thesis number 77
- Kawakami,A., Fukui,K.,Yasutomi,H. and Sato,S. (2009): Ultrasonic borehole scanner (in Japanese), the 121th Conference SEGJ, Proceedings, PP.99-101